FEBS Letters 349 (1994) 289–294

FEBS 14304

Voltage-dependent Ca^{2+} channels in Chinese hamster ovary (CHO) cells

R. Skryma, N. Prevarskaya, P. Vacher, B. Dufy*

Laboratory of Neurophysiology, CNRS URA 1200, University of Bordeaux II, CNRS URA 1200, 146 rue Léo Saignat, 33076 Bordeaux, France

Received 13 May 1994; revised version received 15 June 1994

Abstract

Voltage-dependent Ca^{2+} channels were identified in CHO-K1 cells, currently used in molecular biology studies. Experimental data obtained at both macroscopic and single-channel levels using the patch-clamp technique show that the Ca^{2+} current in CHO cells is similar to the high-threshold L-type of Ca^{2+} current previously observed in excitable cells. It can be carried by Ca^{2+} or Ba^{2+} ions, blocked by both inorganic (Co^{2+}) and organic (nifedipine, isradipine) Ca^{2+} channel blockers. The unitary Ca^{2+} channel activity was characterized by a conductance of 19 pS in 60 mM Ca^{2+}, by single exponential distribution of open times (t = 0.84 ms) and biexponential distribution of closed times (t_f = 1.67 ms, t_s = 7.9 ms). However, the functional role of these Ca^{2+} channels in CHO cells remains unclear.

Key words: CHO-cell; Calcium current; Calcium channel

1. Introduction

Chinese hamster ovary cells (CHO cell line) offer significant experimental advantages in molecular biology studies. As these cells are presumed to have a simple morphology and constant genetic background, they are currently employed for transfection with complementary DNA encoding different receptors, membrane channels and enzymes [1–3]. Most of these studies [4–6] are based on the assumption that CHO-native cells lack voltage-dependent membrane conductances. Moreover, on these assumptions CHO cells were reported to be stably transfected with cDNA encoding various types of ion channels: the R_{IIA} sodium channel rat brain subunit [7], the adenosine 3′,5′-cyclic monophosphate (cAMP)-regulated chloride channel [8], the smooth muscle calcium channel alpha 1 subunit [6] or the rabbit cardiac alpha 1 calcium channel subunit DNA [9]. These preparations were then studied for voltage dependence, unitary current conductance characteristics, and pharmacology of the transfected ion channels. However, chloride [10] and sodium [11] conductances were reported to be present in CHO-native cells. Conversely nothing is known about Ca^{2+} membrane conductance in these cells in spite of the participation of $[Ca^{2+}]_i$ and Ca^{2+} conductances in receptor function mechanisms. CHO cells are reputed to be non-excitable. Mitsuhashi et al. [12] have shown that KCl induced depolarization raised intracellular calcium $[Ca^{2+}]_i$ in CHO cells, indicating the existence of voltage-dependent Ca^{2+} conductance, but to our knowledge the electrophysiological characteristics of the Ca^{2+} conductance(s) of CHO cells have not been studied. In this work we identified the voltage-dependent Ca^{2+} conductance of CHO-K1 cells. The purpose of the present study was to characterize this conductance, which may be important in molecular biology research, ion channel transfections, signal transduction, and which may be activated following binding of receptors expressed in CHO cells with their agonists.

2. Materials and methods

2.1. Cell culture

The chinese hamster ovary (CHO-K1) cells used in these experiments were routinely grown in Ham's F12 medium (Seromed, Strasbourg, France) supplemented with 10% (V/V) fetal calf serum (GIBCO, Grand Island, NY) and incubated at 37°C in a 5% CO_2 humidified environment for at least 24 h before electrophysiological recordings.

2.2. Recording solutions

For whole-cell voltage clamp studies the standard extracellular solution contained (in mM): 140 NaCl, 5 KCl, 10 $CaCl_2$, 2 $MgCl_2$, 0.3 Na_2HPO_4, 0.4 KH_2PO_4, 4 $NaHCO_3$, 5 glucose, 10 HEPES (*N*-2hydroxyethylpiperazine-*N*′-2-ethano-sulfonic acid). The osmolarity of the external salt solution was adjusted to 300–310 mOsmol/kg with sucrose, and pH adjusted to 7.3 ± 0.01 with NaOH. Tetrodotoxin (TTX, 1–5 μM) was added to the bathing solution to prevent activation of the fast sodium current. In some cases, the external solution contained Ca^{2+} as a charge carrier and was composed as follows (in mM): 60 $CaCl_2$, 2 $MgCl_2$, 52.5 TEACl, 10 HEPES/KOH, pH 7.3.

The recording pipette was filled with an artificial intracellular saline containing (in mM): 150 KGlu, 2 $MgCl_2$, 1.1 EGTA (ethyleneglycol bis(b-aminoethyl ether-*N*,*N*,*N*′,*N*′-tetraacetic acid), 5 HEPES (pH 7.3 ± 0.01 with KOH), osmolarity 290 mOsmol/kg. For most experiments in this study potassium gluconate was replaced with isomolar *N*-methylglucamine (NMG) methane sulfonate to eliminate K^+currents, and the pipette solution was supplemented with 3 mM ATP-Mg.

For the study of single calcium channels the cell-attached configuration was used. Some experiments were performed on cell cultures placed in the normal bath solution but to avoid uncertainties in cell resting potential, in some cases, resting potential V_m was zeroed by placing the cells in an extracellular solution containing a high concentration (150 mM) of K^+. For single-channel recordings Ca^{2+} (60 mM) was present in the pipette solution as the permeant cation through the channel, TEA-Cl (52.5 mM), $MgCl_2$ (2 mM), HEPES (10 mM) and TTX (1μM) were also added (pH = 7.3 ± 0.01).

To allow local drug application to the investigated cell an additional 'pouring' pipette with a tip opening of 10–30 μm was used. This pipette was filled with the same extracellular saline as was in the bath and the

*Corresponding author. Fax: (33) 56 90 14 21.

SSDI 0014-5793(94)00690-W

drug under investigation added to it in appropriate concentrations. The pipette was brought close to the investigated cell at a distance of 50–90 μm. All experiments were performed at room temperature (20–22°C).

2.3. Pharmacological reagents

PN 200–110 (Isradipine, Bioblock Scientific, Illkrich, France), Bay K 8644 (Sigma) and nifedipine (Sigma) were dissolved in dimethylsulphoxide (DMSO), divided into aliquots and stored frozen in the dark until use. DMSO in the concentrations used here (< 0.1%) had no effect. Dilution to the final concentration in the external medium was carried out daily under light-protection. ω-Conotoxin was obtained from 'Latoxan' (France), tetrodotoxin (TTX) was obtained from Sigma.

2.4. Electrophysiological recordings

The whole-cell and cell-attached modes of the patch technique were employed. The electrodes were pulled on a L/U-3P (List-Medical, Germany) puller in two stages from borosilicate glass capillaries (Kimax-51, USA) (1.5 mm in diameter) to a tip diameter of 1.5–2.0 μm. Patch electrodes were coated with sylgard and then fire polished. The pipettes had an average resistance of 2–4 MΩ.

The cultures were viewed under phase contrast with a Leitz–Diavert (Leitz, Germany) inverted microscope. Electrodes were positioned with Leitz (Germany) micromanipulators. Grounding was achieved through a silver chloride-coated silver wire inserted into an agar bridge (4% agar in electrode solution).

An Axopatch-1D amplifier (Axon Instruments, USA) was used. Stimulus control and data acquisition and processing were carried out with a PC computer, AT-80386 (Tandon, USA), fitted with a Labmaster TL-1 interface, using Pclamp 5.5.1 software (Axon Instruments, USA - interface and software).

Electrode offset was balanced before forming a giga-seal. Seal resistances were typically in the range of 13–30 GΩ. Leakage and capacitive current subtraction protocols were composed of four hyperpolarizing pulses one-fourth of the test pulse size that were applied from a holding potential before test the pulses. During data analysis, leak data were scaled and subtracted from the raw data. Series resistances were compensated. Series resistances were calculated before and after compensation. The series resistance averaged 1.15 MΩ and ranged from 0.4 to 1.7 MΩ. Recordings where series resistance resulted in a 5 mV or greater error in voltage commands were discarded. Currents were low-pass filtered at 2 kHz (whole-cell) or 1–2.5 kHz (single channel records) with an 8 pole Bessel filter (−3 dB) and digitized at 10 kHz for storage and analysis.

2.5. Data analysis

Peak currents in whole-cell recordings were measured using the automatic peak detection function in the Clampan section of the Pclamp software. Late currents measured isochronally were taken before the end of the pulse to avoid capacitative transients spread out by digital filtering.

Single channel data analysis was performed after elimination of capacity transients and leak current by subtraction of record averages without channel activity from each current record. The openings and closings of the channel were detected using a criterion of a 50% excursion between fully open and fully closed states to determine the occurence of an opening or closing event such as crossings of the line at a half distance between zero current level and a level corresponding to the average open channel amplitude. In this way, real current records were put into ideal form by setting all intermediate amplitudes to the level of zero current line or to the level of the average open channel amplitude. The open probability was calculated as the open time integral divided by the number of channels in the patch and the duration of the data segment analyzed. The number of channels was estimated by examining the record for multiple openings under conditions of high open probability ($P > 0.75$). 10 s data segments were analyzed for open probability estimates.

3. Results

To eliminate K^+ current all the experiments were carried out using NMG substituted solutions. Calcium current in CHO cells was observed in 24% of cells investigated (27 out of 114). Fig. 1 shows families of Ca^{2+} currents obtained from a holding potential −40 mV and the I–V relationships for these currents. In conditions where extracellular solution contained 3 μM TTX (Fig. 1, left) or Na^+ ions replaced by choline (Fig. 1, right), the inward slow inactivating current was observed in response to depolarization pulses of 80 ms duration to membrane potentials between −30 and + 50 mV. In both of these conditions, Ca^{2+} currents evoked with the same voltage protocol were almost the same. Usually the total amplitude of the calcium current in 10 mM external Ca^{2+} concentration was very small. This conductance was no larger in Ba^{2+} than in Ca^{2+}. So, in some recordings the external Ca^{2+} concentration $[Ca^{2+}]o$ was increased to 60 mM.

The co-existence of multiple types of Ca^{2+}-selective channels has been shown in several types of cells [13–15]. These current components were distinguished on the basis of their voltage and time dependencies, ionic selectivity, and pharmacology. We examined the types of calcium current present in CHO cells using the voltage protocol to separate channels exhibiting a low activation threshold from the channel showing a high activation threshold. There was no noticeable difference in the currents evoked when the cell membrane was depolarized from $V_h = -80$ mV and after shifting V_h to −40 mV. Indeed, the threshold (−40 mV) and the potential-dependent parameters of the calcium current observed in

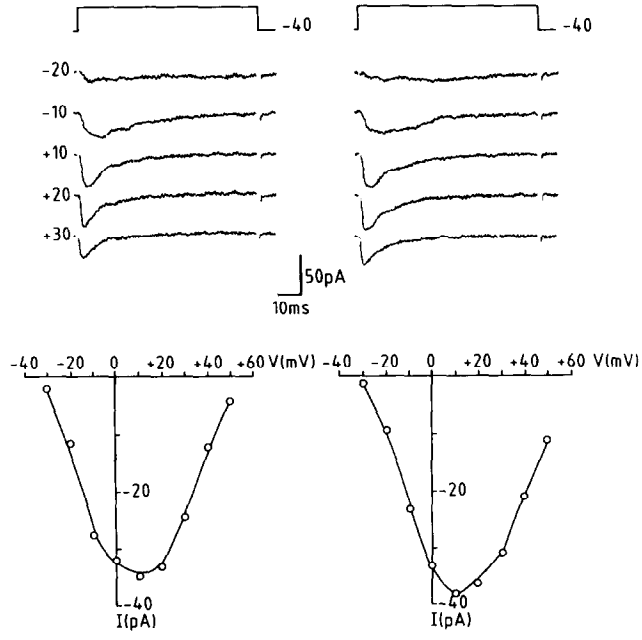

Fig. 1. Calcium currents of CHO cells. Currents evoked by depolarizing pulses to different potentials from the holding potential of −40 mV in the presence of 3 μM TTX (left, top). Currents from the holding potential of −40 mV in the Na^+-free Ca^{2+}-containing solution (right, top). Membrane potentials are shown at the respective current traces. Bottom: I–V curves for the respective currents.

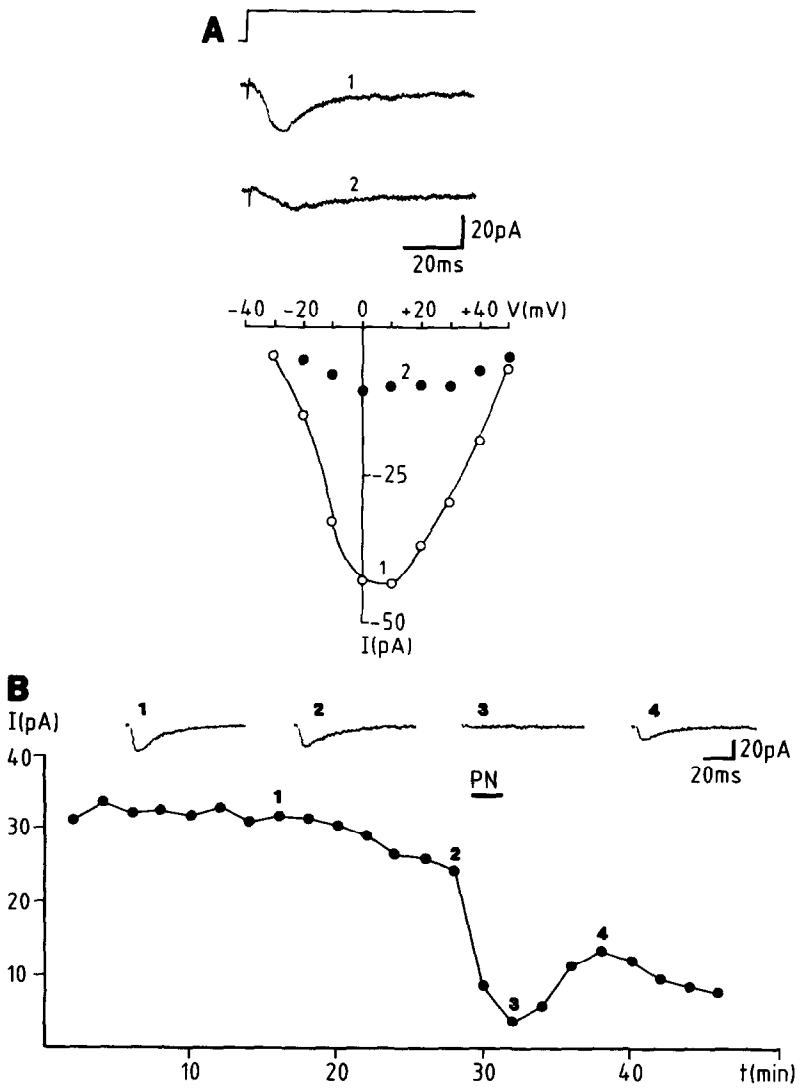

Fig. 2. Ca^{2+}-channel modulators sensitivity of Ca^{2+} current of CHO cells. (A) Co^{2+} action on calcium current in CHO cell. Current records before (1) and after (2) addition of 3 mM Co^{2+} (top). Current records elicited by step depolarizations from −40 mV to −10 mV. Peak current levels before (1) and after (2) addition of Co^{2+} are plotted against the membrane potential (bottom). (B) Isradipine action on calcium current of CHO cell. Current traces obtained before (1,2), after 50 nM isradipine adding (3) and after washout (4). Currents were evoked by 80 ms test pulses from holding potential of −40 mV to +10 mV. The respective plot of peak current versus time is shown below.

CHO cells correspond to those of the high-threshold calcium current previously described in other cell types.

Experiments were carried out to test the sensitivity of the Ca^{2+} current to pharmacological agents, namely Co^{2+}, nifedipine, isradipine (PN-200–110), ω-conotoxin. In 7 experiments, Ca^{2+}-channel blocker Co^{2+} (3 mM) (Fig. 2A) was added to the solution bathing the cells and caused both a reduction in Ca^{2+} current amplitude and also a weak shift (approximately 10 mV) of the I–V curve toward more positive potentials. Ca^{2+} current in CHO-K1 cells was also sensitive to dihydropyridines. Dihydropyridines reduced Ca^{2+} current in a dose-dependent manner without shifting the I–V curve. 10 μM nifedipine reduced Ca^{2+} currents by 20–30% (5 experiments); 50 μM reduced Ca^{2+} currents by 70% (4 experiments) and 100 μM reduced Ca^{2+} currents by 80–90% (5 experiments) at all applied voltages. Isradipine was even more efficient in inhibiting the Ca^{2+} current in CHO cells. 10 nM isradipine reduced Ca^{2+} currents by approximately 50% (6 experiments) and 100 nM isradipine completely abolished inward currents at all voltages (5 experiments). Fig. 2B shows an example of Ca^{2+} current inhibition induced by 100 nM of isradipine. Isradipine reversibly decreased the Ca^{2+} current. The sensitivity of this current to Ca^{2+} agonist BAY K 8644 was much lower than usual for dihidropyridine-sensitive Ca^{2+} channels. 1–5 μM BAY K 8644 increased the amplitude of the Ca^{2+} current by no more than 10 ± 5% (7 experiments). ω-conotoxin was ineffective (data not shown), indicating that the N-component of the high-threshold Ca^{2+} current was absent in CHO cells.

The Ca^{2+} current was not stable under internal perfu-

sion (e.g. Fig. 2B). If membrane potential was stepped up to +10 mV for 80 ms at intervals of 1 or 2 min, the magnitude of the Ca^{2+} current decreased with time. Fig. 2B shows calcium current rundown during intracellular perfusion of CHO cell as obtained in the whole-cell configuration. Within an hour after rupture of the seal and dialysis of the cytoplasm using saline solution, the Ca^{2+} current had almost completely disappeared. This was not due to a general deterioration of the cell, because the capacitance of the cell did not change and the leakage current remained stable throughout perfusion.

Cell-attached configuration was used for single channel recordings. After formation of a giga-seal between the membrane and the tip of the recording pipette in conditions where all types of ion channels except calcium were suppressed, calcium single channels could be recorded in 39% of patches investigated (9 out of 23). There was no basic variation from one patch to another in the characteristics of activity observed using Ca^{2+} or Ba^{2+} as a charge carrier. Fig. 3A presents examples of activity recorded during test pulses from a holding potential of −40 mV to a test potential of −10 mV (left panel) and +10 mV (right panel), using 60 mM Ca^{2+} as the charge carrier. The same single Ca^{2+} channel behavior was also preserved after zeroing of V_{rest} by high external K^+. Detailed examination of experimental current records has shown that all these observations resulted from the functioning of one type of calcium channel. Current pulses started to appear at depolarization to −30 mV. Further depolarization increased their open probability. From the I–V relationship, single channel slope-conductance was estimated to be about 18 pS (data not shown). The amplitude histogram of Ca^{2+} channel activity at a membrane potential of +10 mV is presented in Fig. 3B. The channel's activation and inactivation kinetics were consistent with those of the current, obtained from whole-cell recordings under the same ionic conditions. The analysis of the open- and closed-time kinetics is shown in Fig. 3C. Open-time distribution fit a single exponential with a time constant of 0.84 ms, suggesting the existence of a single open-state for this channel. On the other hand the closed-time distribution fit double exponentials, with a fast time constant of 1.67 ms and a slow time constant of 7.9 ms, suggesting that there are at least two closed-states.

Fig. 4 shows the effect of 50 nM isradipine on single

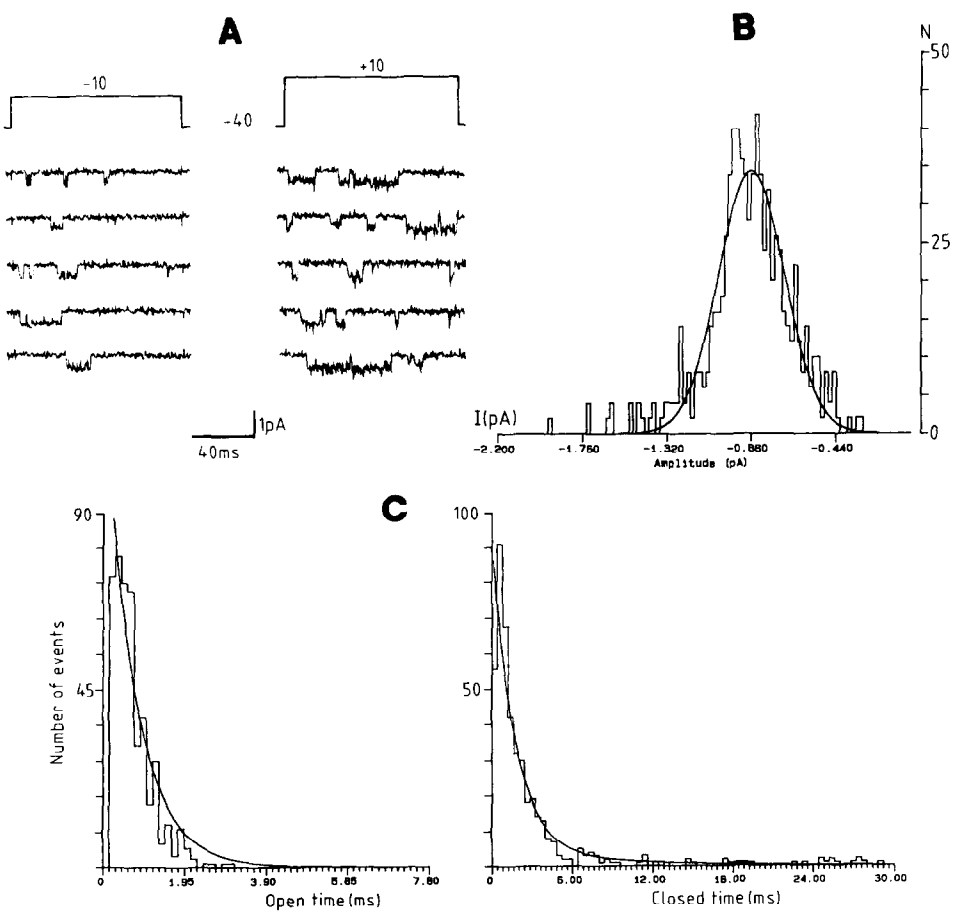

Fig. 3. Activity of single Ca^{2+} channels of CHO-K1 cell. (A) Examples of original current records obtained in cell attached configuration in response to two successive depolarizations. (B) Amplitude histogram of Ca^{2+} channels for +10 mV membrane potential. (C) Left: open time distribution, the smooth curve is a single exponential with t = 0.84 ms (total number of events n = 465). Right: closed time distribution fit the sum of two exponentials with the time constants t_f = 1.67 ms, t_s = 7.9 ms (total number of events n = 454).

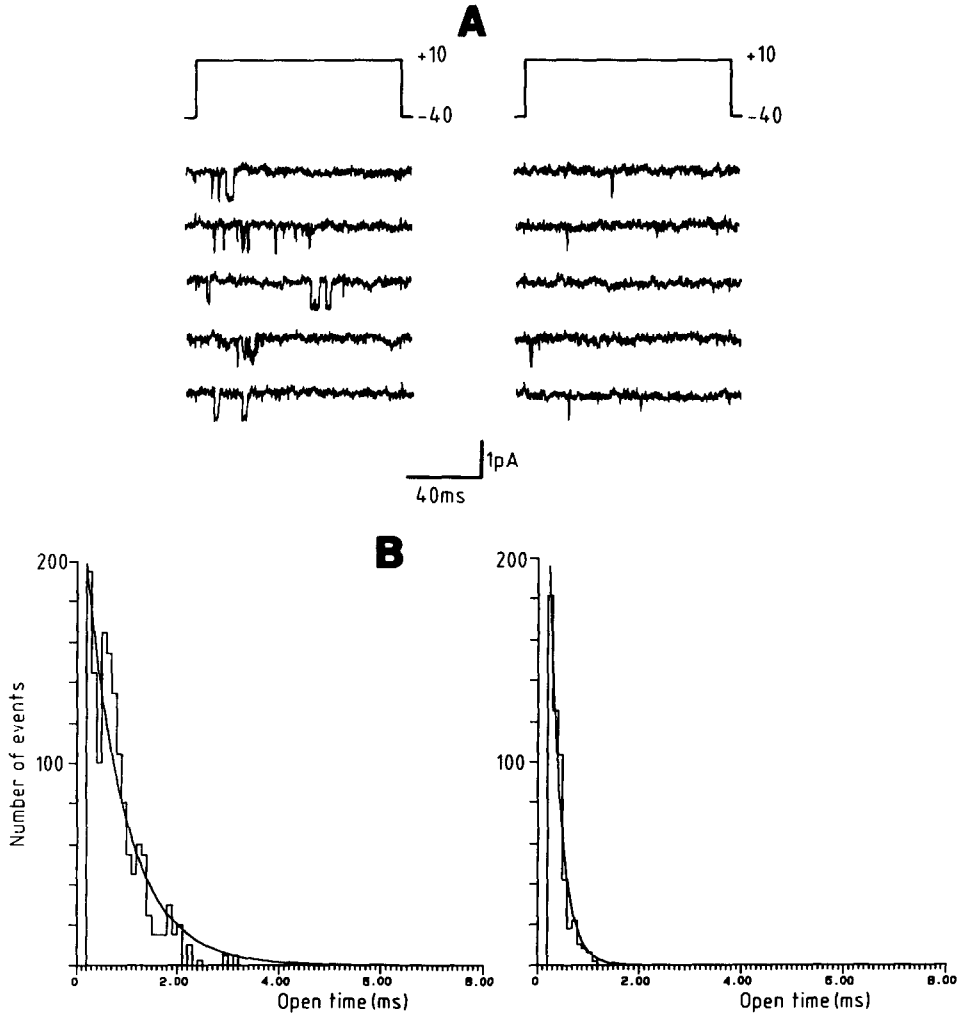

Fig. 4. Action of 50 nM isradipine on single Ca^{2+} channels of CHO cells. (A) Original Ca^{2+} current records induced by the step to +10 mV from −40 mV (left) and the records with the same voltage protocol from the same patch 3 min. after adding 50 nM isradipine to the bathing solution. (B) Histograms of open times before (left) and after (right) application of isradipine. Smooth lines: single exponential fit of experimental histograms with time constants $t = 0.79$ ms ($n = 574$) for the control and $t = 0.24$ ms ($n = 260$) after adding isradipine, respectively.

Ca^{2+} channel activity at a membrane potential of +10 mV (Fig. 4A) and open-time distribution of Ca^{2+} channels (Fig. 4B) in CHO cells. The time constant of the open time histogram decreased from 0.79 ms to 0.24 ms with isradipine.

4. Discussion

These experiments directly demonstrate the presence of a voltage-dependent Ca^{2+} current in CHO-cell membrane. Ca^{2+} ions were responsible for the inward membrane currents evoked by membrane depolarization in the presence of TTX. Under these conditions, inward currents were not observed in the absence of extracellular Ca^{2+} but were enhanced when the extracellular Ca^{2+} concentration was increased, and they were blocked by both inorganic and organic Ca^{2+}-channel blockers.

We could not find any evidence for the presence of multiple types of Ca^{2+} channels in CHO cells. No other Ca^{2+} currents were disclosed by two studies using conventional voltage-clamp protocols [16,18] to identify a low-threshold component of Ca^{2+} current and pharmacological experiments with ω-conotoxin that specifically blocks N-type of Ca^{2+} current [19,20]. Moreover, nifedipine (100 mM) and isradipine (100 nM) completely blocked Ca^{2+} current, indicating the presence in CHO cells of a single type of dihydropyridine-sensitive Ca^{2+} current. This current is similar to the high-threshold L-type of Ca^{2+} current previously described in many systems [14,18,21,22], except for some properties that distinguish it from the known types of Ca^{2+} channels. First, there was no significant difference in activation voltage dependencies, time to peak or inactivation between Ca^{2+} and Ba^{2+} currents, while L-type Ca^{2+} current is usually more selective for Ba^{2+} than for Ca^{2+} ions [16]. Second, Bay K 8644 (10 nM–1 μM), known as an agonist of dihydropyridine-sensitive Ca^{2+} channels, did not pro-

duce any obvious effect on the Ca^{2+} current in CHO cells during whole-cell and single-channel experiments. However, similar observations were reported for Ca^{2+} channel L-type current in Purkinje fibres [23] and ventricular cells [24]. Third, the inactivation of Ca^{2+} current in CHO cells is more rapid than that of the classical slowly inactivating L-type Ca^{2+} current [25]. Finally, the rundown of Ca^{2+} current in CHO cells is slower than in other cell types (in our experiments, the rundown to half of the initial calcium current amplitude took about 30–40 min, while in most cell types it takes about 15–20 min [21,26]). Currents that do not fit neatly in the known calcium current classifications 'L,T,N,P....' were also demonstrated [27].

In single-channel experiments, we found that the unitary conductance of Ca^{2+} channels in 60 mM Ca^{2+} solution is 19 pS, similar to that of exitable cells [13]. The amplitude histogram distribution confirms the existence of a single type of Ca^{2+} channel. This channel has a single exponential open time distribution and biexponential closed time distribution for all test potentials. This type of distribution reflects the presence of one open (conducting) state and two closed states with different lifetimes for Ca^{2+} channels in CHO cells. This kinetic distribution was very similar to those already described for high-threshold L-type Ca^{2+} current in various cell types [14,16,17]. However, other studies involving pheochromocytoma cell lines showed a biexponential open time distribution [16].

CHO cells are presumed to belong to a clonal cell line showing constant features, however calcium currents were only observed in 24% of cells investigated. The reason for these differences in cell responses is not known. As CHO cells are fast growing, we may have recorded cells at different stages in the cell cycle and one hypothesis is that these channels are not uniformly expressed during the cell cycle.

References

[1] Penner, R., Neher, E., Takashima, H., Nishimura, S. and Numa, S. (1989) FEBS Lett. 259, 217–221.
[2] Piomelli, D., Pilon, C., Giros, B., Sokoloff, P. and Martres, M.P. (1991) Nature 353, 164–167.
[3] Numann, R., Catteral, N.A. and Scheur, T. (1991) Science 254, 115–118.
[4] Jones, S.V. (1993) Life Sci. 52, 457–464.
[5] Robertson, B. and Owen, D.G. (1993) Br. J. Pharmacol. 109, 725–735.
[6] Boss, E., Bottlender, R., Kleppish, T., Hescheler, J., Welling, A., Hofmann, F. and Flockerzi, V. (1992) EMBO J. 11, 2033–2038.
[7] Scheuer, T., Auld, V.J., Boyd, S., Offord, J., Dunn, R. and Catterall, W.A. (1990) Science 247, 854–858.
[8] Tabcharani, J.A., Chang, X.B., Riodan, J.R. and Hanrahan, J.W. (1991) Nature 352, 628–631.
[9] Yoshida, A., Takahashi, M., Nishimura, S., Takeshima, H. and Kokubun, S. (1992) FEBS Lett. 309, 343–349.
[10] Gabriel, E.S., Price, E.M., Boucher, R.C. and Shutts, M.J. (1992) Am. J. Physiol. 263, C708–C713.
[11] Lalik, P.H., Krafte, D.S., Volberg, W.A. and Ciccarelli, R.B. (1993) Am. J. Physiol. 264, C803–C809.
[12] Mitsuhashi, T., Morris, R.C. and Ives. H.E. (1989) J. Clin. Invest. 84, 635–639.
[13] Kostyuk, P.G., Shuba, Y.M. and Savchenko, A.N. (1988) Pflügers Arch. 411, 661–669.
[14] Yoshino, M., Someya, T., Nishio, A., Yazawa, K., Usuki, T. and Yabu, H. (1989) Pflügers Arch. 414, 401–409.
[15] Fox, A.P., Nowycky, M.C. and Tsien, M.C. (1987) J. Physiol. 394, 149–172.
[16] Kostyuk, P.G., Shuba, Y.M., Savchenko, A.N. and Teslenko, V.I. (1988) In: The Calcium Channel: Structure, Function and Implications (Morad, Nayler, Kazda and Schramm Eds.) pp. 442–464, Springer-Verlag, Berlin.
[17] O'Dell, T.J. and Alger, B.E. (1991) J. Physiol. 436, 739–767.
[18] Nowycky, M.C., Fox, A.P. and Tsien, R.W. (1985) Nature 316, 440–443.
[19] Oyama, Y., Tsuda, Y., Sakakibara, S. and Akaike, N. (1987) Brain Res. 424, 58–64.
[20] Scroggs, R.S. and Fox, A.P. (1992) J. Neurosci. 12, 1789–1801.
[21] Savtchenko A.N. and Verkhratsky, A.N. (1990) Gen. Physiol. Biophys. 9, 147–166.
[22] Skryma, R.N., Prevarskaya, N.B. and Burdyga, P.V. (1989) Neurophysiology 21, 261–264.
[23] Sanguinetti, M.C., Krafte, D.S. and Kass, R.S. (1986) J. Gen. Physiol. 88, 369–392.
[24] Hess, P., Lansman, J.B. and Tsien, R.W. (1984) Nature 311, 538–544.
[25] Eckert, R. and Chad, J.E. (1984) Prog. Biophys. Mol. Biol. 44, 215–267.
[26] Fedulova, S.A., Kostyuk, P.G. and Veselovsky, N.S. (1985) J. Physiol. 359, 431–446.
[27] Przysiezniak, J. and Spencer, A.N. (1992) J. Neurosci. 12, 2065–2078.